Background understanding and rejection for CCD dark matter searches using DAMIC at SNOLAB

Elise Darragh-Ford
Department of Astronomy
University of Chicago
Chicago, IL 60637
edarraghford@uchicago.edu

June 3, 2019

Abstract

For the DAMIC (DArk Matter In CCDs) experiment, background events from radioactive decays place the largest limit on direct detection sensitivity. Thus, characterizing and eliminating this type of background is essential to the success of the experiment. The work presented here tackles both sides of this problem using data from a previous run of DAMIC at SNOLAB. The background from radioactive contamination of detector components is characterized using simulated spectra in order to set a baseline for background rates. We also develop analysis methods to identify and reject the background from ^{32}Si, of cosmogenic origin, using a coincidence search, which takes advantage of the spatial correlation between the two β decays in the ^{32}Si - ^{32}P decay chain. By combining this ^{32}Si coincidence search with methods for physically eliminating the other dominant background components during the process of manufacture, transport, and installation, we hope to reduce background levels below 0.1 dru in the next generation of DAMIC (DAMIC-M), set to run in the Laboratoire Souterrain de Modane. Thus, this analysis is integral to achieving the high levels of sensitivity necessary to the future success of the DAMIC experiment.

1 Introduction

The DAMIC (DArk Matter In CCDs) experiment employs novel techniques in the field of dark matter direct detection searches. Today, it is widely accepted that dark matter makes up over 80% of matter in the universe [1]. However, scientists have yet to discover which particles are responsible for this mysterious extra mass. The leading theory is that dark matter is made up of Weakly-Interacting Massive Particles (WIMPs), which interact only weakly with standard matter [2]. Although this makes them a compelling candidate for dark matter, it introduces serious challenges for direct detection. The DAMIC experiment attempts to measure these WIMPs using super-sensitive silicon charge coupled-devices (CCDs). The theory is that although WIMPs do not interact with normal matter through any force stronger than the weak nuclear force, they can still occasionally collide directly with the nucleus of an atom. This process, called coherent elastic scattering, will induce a recoil of the nucleus which can then be detected. By using silicon CCDs as the target for these nuclear recoils, DAMIC can measure coherent WIMP-nucleus elastic scattering at keV energy scales. This is because the low pixel readout noise and low leakage current of the detectors make DAMIC extremely sensitive to ionization signals from the interaction of dark matter particles with nuclei or electrons in the bulk silicon of the CCDs. Additionally, the low mass of the silicon nucleus provides a good sensitivity to WIMPs with masses in the range 1-10 GeV/c^2, while the small band gap of silicon provides sensitivity to dark matter-electron interactions that deposit as little as 1.1 eV in the target [2]. This low energy sensitivity means that DAMIC is also sensitive to more exotic types of "light" dark matter particles, which have recently been proposed in the absence of a robust WIMP signature detection, which would interact with the electrons rather than the nuclei of an atom.

However, achieving the required sensitivity for direct detection is still challenging, due to background caused by radioactive decays. These backgrounds turn out to place the largest limit on direct detection sensitivity because nuclear decays can occur at approximately the same energy scales as predicted WIMP nuclear recoils. Thus, finding methods to
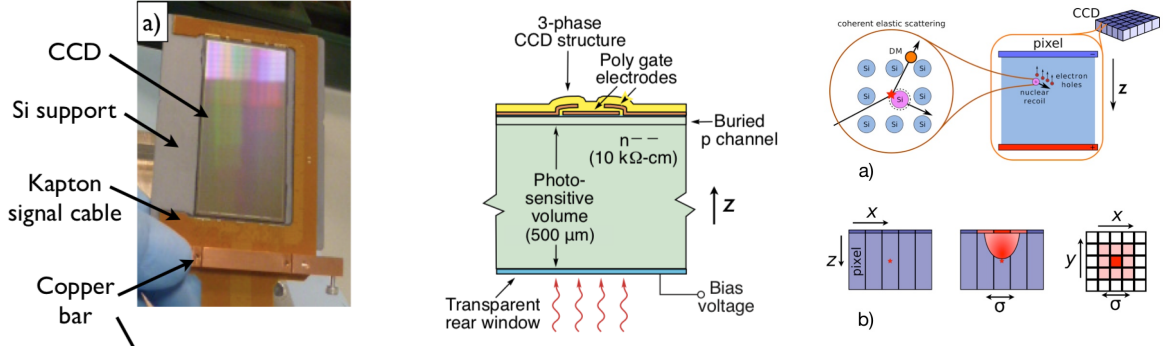
Figure 1: A packaged DAMIC CCD with kapton cable and CCD detector labeled (*left*). A CCD pixel showing bulk silicon, bias voltage, and readout channel (*center*). Mechanism of WIMP detection in a CCD pixel. In part a, a dark matter particle is seen colliding with the Si nucleus creating electrons and holes which are then drifted to CCD pixel. Part b shows the process of diffusion whereby charges created at some depth z in the CCD, diffuse radially, creating distinctive circular regions of charge in the x-y plane of the pixel and allowing for depth reconstruction (*right*). [3]

eliminate these backgrounds is essential to the future success of the DAMIC experiment. To lower these backgrounds, the DAMIC detectors are shielded using ancient lead and placed underground. The DAMIC experiment is currently taking data in the SNOLAB underground laboratory in Sudbury, Canada with an approximately 40g detector [2]. The upcoming kg-size DAMIC-M experiment will be installed at the Laboratoire Souterrain de Modane, which is located underneath the Alps in France. By placing the CCDs deep underground and using shielding materials, we are able to eliminate most of the cosmogenic radioactive background. However, the various detector components themselves still experience radioactive contamination during the process of manufacture, transport, and installation. Characterization of these backgrounds is essential to performing proper analysis on the data from DAMIC at SNOLAB and to determining whether the DAMIC-M experiment will meet required sensitivity limits. In this analysis, I focus on characterization and elimination of these backgrounds in DAMIC at SNOLAB.

1.1 Detector Setup

For DAMIC at SNOLAB, the detector consists of seven working high-resistivity, fully depleted, silicon CCDs (extensions 1, 2, 3, 4, 6, 11, 12), weighing about 6.0g each. Each device consists of 4116 pixels in x and 4128 pixels in y, with a pixel size of (15×15) μm^2 and a thickness of $675 \mu m$. For the 1x100 data, considered here, columns of charge 100 pixels high are stacked before being readout in order to speed up the readout time and reduce the effect of readout noise. Each CCD is epoxied onto a silicon backing, together with a flex cable that is wire bonded to the CCD and provides the voltage biases, clocks and video signals required for its operation. These components are supported by an OFC copper frame to complete the CCD module (Fig 1). The modules are installed in a copper box that is cooled to 140 K inside a vacuum chamber. The box is shielded by 18 cm of lead to attenuate external γ rays, with the innermost 2 inches made of ancient lead, and by 42 cm-thick polyethylene to moderate and absorb environmental neutrons [2]. By using ancient lead (from a recovered Roman ship) we eliminate background from the β decay of ^{210}Pb ($\tau_{1/2} = 22.3$ years).

The CCDs themselves feature a three-phase polysilicon gate structure with a buried p-channel (Fig 1). To be read out, energy deposited in a pixel by an incoming particle is drifted to the pixel array by an electric field, induced by the bias voltage which normally operates at Vsub = 70 V. As the charge is drifted up through the CCD, it diffuses (Fig 1). By analyzing the amount and pattern of diffusion, we can accurately reconstruct the three dimensional position of the energy deposit, and from this, identify the type of particle based on the charge distribution pattern (Fig 2). This type of distribution pattern analysis can be used to identify higher energy electrons (e) (from Compton scattering or beta decays), which leave a curly "worm-like" track, cosmic muons (μ), which leave a long straight track, as well as alpha decays (α) occurring on either the front (bloomed) or the back (plasma) of the CCD, which leave distinctive blob shapes (Fig 2) [3]. However, these methods break down when trying to identify lower energy, diffusion limited events. At these energies there is not enough information in the shape to distinguish the signature of a WIMP interaction from a low energy β decay or X-ray. Thus, other analysis methods are required. Once the charge has been moved to the pixel array, the CCD is then readout line by line.
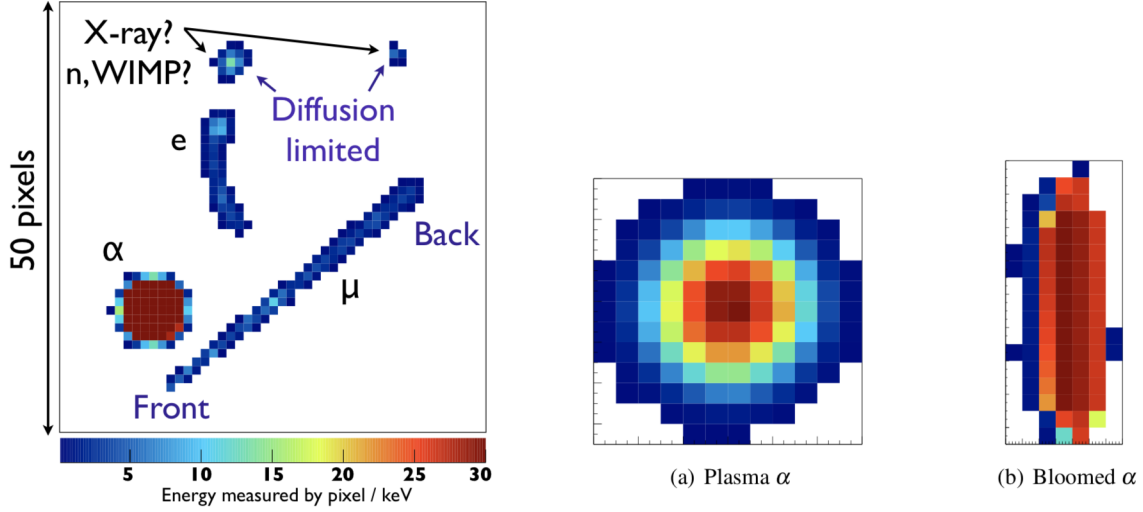
Figure 2: Examples of various types of particles that can be identified in the CCDs using analysis of charge diffusion patterns (*left*). Pattern of α particle originating in either the back (plasma) or front (bloomed) of the CCD (*right*). [3]

1.2 Background

Radioactive contamination during the process of manufacture, transportation, and installation can occur in all components of the DAMIC detector setup. However, the detector parts which we have determined contribute most significantly to the overall background in DAMIC at SNOLAB, and are predicted to be the dominant components in DAMIC-M as well, are the CCDs themselves, the copper modules, and the flex cable as these are the components operating closest to the actual detector arrays. Previous studies have shown that the other components contribute at levels below the required sensitivity threshold for operation, and thus are excluded from this analysis. The radioactive decay chains that prove most important are those that we expect to be present in the above components and have isotopes with long half-lives, meaning they are likely to exist in any material we procure, and have Q values similar to the energy scales important in the WIMP search. The decay chains we consider in this analysis are ^{32}Si, ^{210}Pb, ^{238}U, ^{226}Ra, ^{232}Th, ^{40}K, ^{22}Na, ^{3}H, and activation of copper (Activation) with the specific isotopes, Q-values, and half-lives specified in Table 1. The copper activation is due to cosmic-ray interactions with the material which produce radioactive nuclei through spallation. Tritium (^{3}H) is produced in the bulk silicon of the CCDs by the same process.

In order to achieve the desired sensitivity of DAMIC-M, we aim to get the background levels down to < 0.1 dru (counts/kev/kg/day) in the low-energy part of the spectrum. This can be achieved through a variety of different approaches. The most straightforward approach is to physically eliminate the contamination from the various components (Section 4.1). However, for some components, physically removing the contamination can prove difficult to impossible, for instance ^{32}Si contamination in our bulk silicon. This is due to the fact that ^{32}Si is produced by cosmic ray interactions with nuclei in the atmosphere. It is then brought to the ground by rain where is becomes part of the sand, which is the raw material used for the fabrication of silicon detectors. Thus, in this instance, we rely on data analysis methods for determining and eliminating erroneous signals. This will be described further in Section 3.2.

2 Data Used

2.1 Geant4 Simulation Dataset

To determine which backgrounds are most important in our specific setup, we start with activity limits based on measurements performed upon our current detector components. We use these measurements to set bounds on the levels of contamination currently present in the DAMIC detector setup at SNOLAB. Then, using a model detector setup and these contamination limits, we simulate the spectra we expect to see in each of the CCDs for each of the individual decay chains and detector components. The simulated model of the detector at SNOLAB is made up of 190 volumes, 74 of which are unique. The decay spectra simulations are generated using the CERN particle simulation platform, Geant4 [6], which is designed to produce radioactive isotopes by volume. In total, 23 isotopes have been simulated

Table 1: Decay Chain Table [4] [5]

Decay Chain	Isotope	Q-Value (keV)	Half-Life
^{238}U	^{234}Pa	2194	6.7 h
	^{234}Th	274	24.1 d
^{226}Ra	^{214}Pb	1018	27.1 m
	^{214}Bi	3269	19.9 m
^{210}Pb	^{210}Pb	63.5	22.2 y
	^{210}Bi	1161.2	5.0 d
^{232}Th	^{228}Ac	2123.7	6.15 h
	^{228}Ra	45.5	5.8 y
	^{212}Pb	569.1	10.6 h
	^{212}Bi	2251.5	60.6 m
	^{208}Ti	4998.5	3.1 m
^{40}K	^{40}K	1310.9	1.2×10^9 y
Activation	^{56}Co	2132.9	77.2 d
	^{57}Co	3261.7	271.7 d
	^{58}Co	381.6	70.7 d
	^{60}Co	2822.8	5.3 y
	^{59}Fe	1564.9	44.5 d
	^{54}Mn	696.9	312.2 d
	^{46}Sc	2366.6	83.8 d
^{32}Si	^{32}Si	227.2	153 y
	^{32}P	1710.7	14.3 d
^{3}H	^{3}H	18.6	12.3 y
^{22}Na	^{22}Na	4781.6	2.6 y

within the bulk of the different volumes. However, not all of these make a large enough contribution to the background to be included in this analysis.

2.2   SNOLAB 1x100 Dataset

The data used for the coincidence search is 1x100 data taken from the DAMIC at SNOLAB experiment. Data acquisition began 2017/09/27 and ended 2018/12/18. After making cuts for runs with uneven leakage current and images that were affected by problems in the data acquisition, the data set consists of 6048 images from 864 exposures for a total exposure time of 273 days. The images are then processed using reconstruction code which was previously developed by researchers in the collaboration.

3   Analysis Tools

3.1   GUI

In order to determine which backgrounds we need to focus on lowering to achieve our desired sensitivity for DAMIC-M, we first need to understand the most significant backgrounds in our current setup at SNOLAB. In order to do this, I developed a graphical user interface (GUI), which allows its user to access the various simulated decay chains and components and display the normalized spectra in dru for a specified energy range. In order to go from the Geant4 spectrum, which is in total number of interactions per bin, to a rate in dru (events/kg/kev/day), the spectrum is normalized according to Equation 1.

$$\text{rate (dru)} = \frac{(\text{interactions})(n_{bins})(\text{A}_{iso})(\text{m}_{comp})}{(\Delta E)(N_{decays})(\text{M}_{CCD})} \tag{1}$$
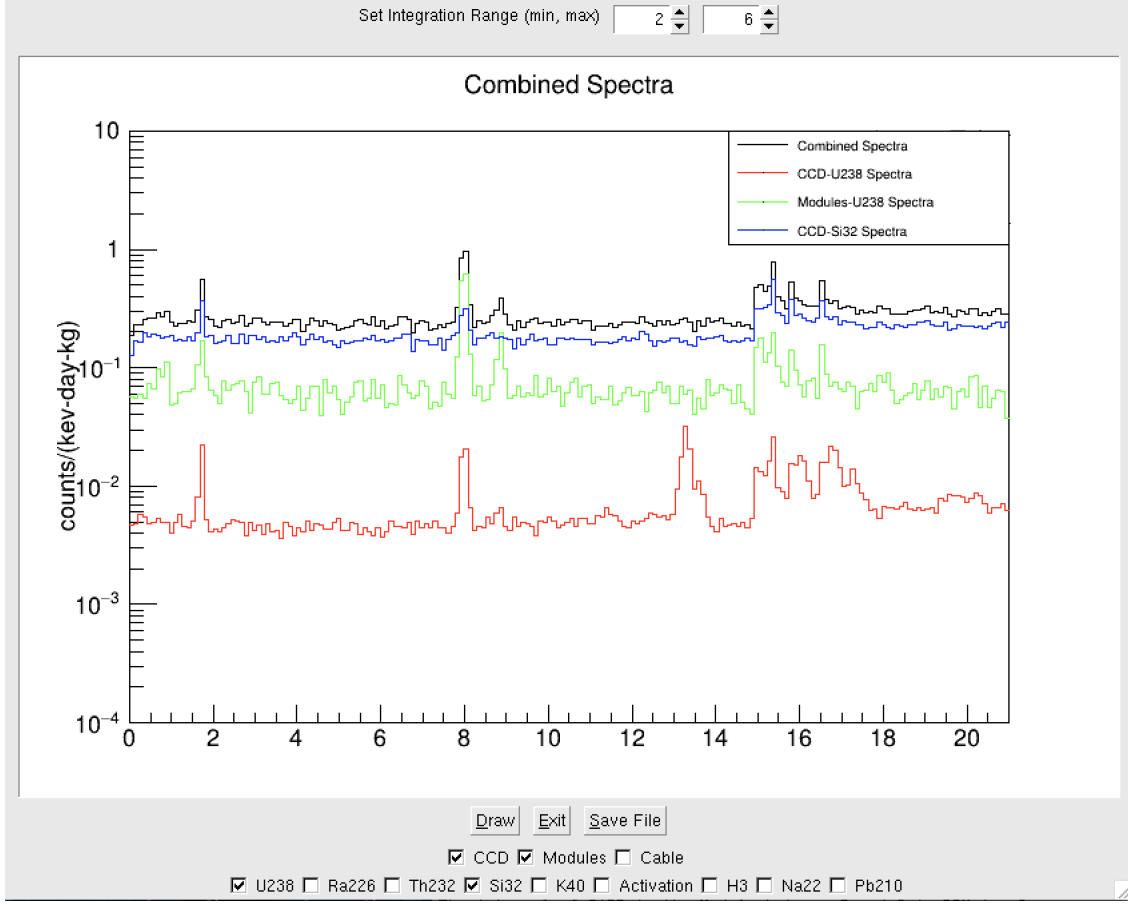
Figure 3: Example of GUI plot for the ^{238}U and ^{32}Si background in the CCD and the copper modules.

where n_{bins} is the number of bins in the histogram, A_{iso} is the activity of the isotope in decays/kg/s, m_{comp} is the mass of the specific component in kg, ΔE is the energy range of the plot, normally set to 0 - 21 keV, and M_{CCD} is the mass of a single CCD (0.00583 kg). This allows us to generate a spectrum in dru.

The GUI allows the user to specify which components and decay chains to view, and the integration range over which to determine the background rate in dru of each decay chain and component specified. It then returns a normalized plot of the various spectra selected, which can then be saved to a ROOT [7] file, along with a readout of the individual and overall background rates. Since each component consists of many different volumes in Geant4 and each decay chain multiple different isotopes, the creation of a GUI allows for component-by-component analysis of the different background contributors without needing to manually select which spectra to view from hundreds to thousands of component simulations. Thus, the GUI significantly speeds up this type of analysis across the collaboration and reduces the likelihood of user-induced error. Additionally, it is easy to update as new components and decay chains are simulated (Fig 3).

3.2 Coincidence Search

Since it is not feasible to physically remove the ^{32}Si from the detectors, removal of the ^{32}Si decay chain background must be done through analysis methods. Previous work done by the DAMIC collaboration has given strong indication that this can be achieved using methods which exploit the spatial and temporal relationship between the two β decays in the ^{32}Si - ^{32}P decay chain [3]. The ^{32}Si - ^{32}P-^{32}S decay chain consists of of two β decays culminating in the stable ^{32}S isotope. The half-lives and Q values for these decays can be found in Table 1. In this note, we extend this previous analysis to the most recent 1x100 data taken with DAMIC at SNOLAB. In order to find ^{32}Si decay events, we search for correlations in our data between two events occurring in the same CCD with endpoints within 7 pixels of each other. The two events must also share at least one pixel of overlap. Additionally the following energy and time separation cuts
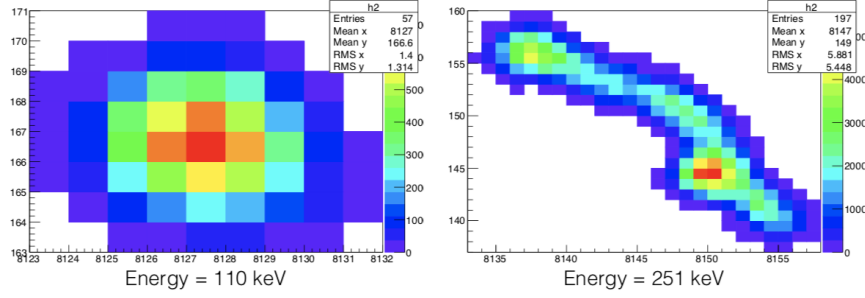
Figure 4: Example of a candidate ^{32}Si β decay pair. The time separation between these two events is 10 days.
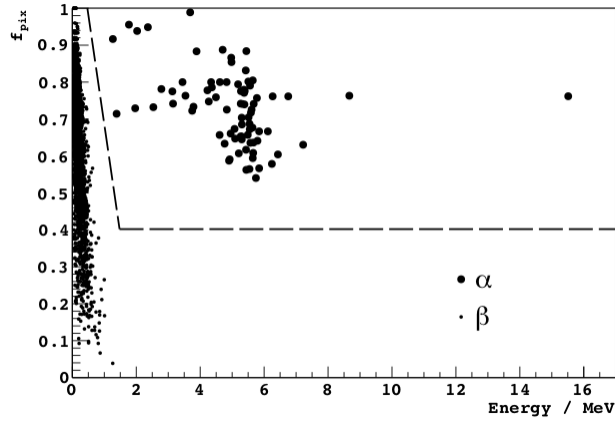

Figure 5: α-β selection using the fraction f_{pix} as a function of the cluster energy. Clusters in the region above the dashed line are selected as αs.

are applied based on the Q value and half-life of the ^{32}Si - ^{32}P decay:

$$\text{Region 1: } \{\text{decays} \,|\, (70 < E_1 \text{ (keV)} < 230), (t_{sep} \text{ (days)} < 70)\}$$
$$\text{Region 2: } \{\text{decays} \,|\, (E_1 \text{ (keV)} < 70), (25 < t_{sep} \text{ (days)} < 70)\} \tag{2}$$

where E_1 refers to energy of the first decay in the decay pair, and t_{sep} is the number of days separating the two events. The spectrum search is performed in two regions, region 1 and region 2, in an attempt to avoid potential contamination from coincident ^{210}Pb decays, which occur with a Q value of 63.5 keV and a half-life of 5 days and are expected to also contribute significantly to the radioactive background. An example of a candidate decay pair for region 1 is shown in Figure 4.

Since the ^{32}Si and ^{32}P decays are both β decays, we also the require that neither event in the pair is identified as an alpha particle. Alpha particles lose most of their energy through ionization, which creates dense regions of electron-hole pairs. This leads to distinctive blob shaped tracks in the CCD. Meanwhile, in the energy range of these radiogenic α particles, electron tracks are long and deposit their energy over many CCD pixels (Section 1.1). Thus, to differentiate electrons from αs, we determine the smallest rectangular box that can contain a cluster, and compute the fraction of pixels, f_{pix}, in this "bound box" which are part of the cluster. For small, symmetric clusters (i.e. αs) f_{pix} is large ($\pi/4$ for a round cluster). For the long and irregularly shaped worms characteristic of electrons, f_{pix} is small and decreases with increasing electron energy. Figure 5 shows the successful separation between βs and αs in a previous analysis done by the DAMIC collaboration [3]. When applied to the 1x100 dataset, these cuts remove 14 potential coincidence pairs from our analysis.

In order to return a rate for each of the regions in events/kg/day, from the raw number of events detected, we utilize Equation 3.

$$\text{rate}_i = \frac{(n_{i\,\text{events}} - n_{i\,\text{accidentals}})}{(p_{i\,\text{detection}})(p_{i\,\text{spectrum}})(p_{\text{efficiency}})(m_{CCD})(t_{total})} \tag{3}$$

6

Table 2: Values Used for Coincidence Search for the Two Separate Regions [8]

	Region 1	Region 2
$p_{detection}$	55.8%	14.4%
$p_{spectrum}$	44.3%	55.7%

First we start with the total number of coincident events ($n_{i\,\text{events}}$), then we subtract off the estimated number of "accidental" coincidences ($n_{i\,\text{accidentals}}$). The number of accidentals is calculated by taking all the events in a CCD and spatially scrambling them, then repeating the same analysis. This number is averaged over 10 trials in order to smooth out statistical fluctuations. This gives us an estimate of how many of these "pairs" we would expect to find if the events were distributed randomly, rather than actually being a part of one of these spatially correlated decay chains. The values for the total number of events and accidentals for each of the two searches is given in Table 5. We then have to correct for the efficiency of detection ($p_{detection}$). This accounts for the fact that the detectors do not take data continuously throughout the entire run, and thus there are gaps in the data between exposures where decays could have occurred and been missed in the current analysis. It also accounts for the fact that the probability of decay decreases as time increases; this is accomplished by defining a starting point at the beginning of each run, and then integrating all future runs against the exponentially decreasing probability that a decay occurs during the time period of that run given the half-life of the isotope under consideration (14.3 days for ^{32}Si). Additionally, we divide by $p_{spectrum}$, which takes into account the percentage of the ^{32}Si decay energy spectrum accounted for in each of the two searches. The values used in this analysis for each of the two regions can be found in Table 2.

From this we have a value for the total number of decays for each of the two regions. We then have to correct for the efficiency to identify a ^{32}Si decay chain ($p_{efficiency}$). This was determined by performing the same analysis on a set of Monte Carlo data simulated with Geant4. Thus, it also takes into account the efficiency of the search parameters, including the requirement of a one pixel overlap and a less than seven pixel displacement. The values used in this section of the analysis are reported in Table 3. We then divide by the mass of the CCDs (m_{CCD}) and the total number of days of data collection (t_{total}). From this we determine a rate of decay in events/kg/day for each of the regions considered.

The error can be calculated assuming a Poisson distribution for the number of events and number of accidentals, and thus goes as the square root of n:

$$\text{err}_i = \frac{(n_{i\,\text{events}} + n_{i\,\text{accidentals}})^{1/2}}{(p_{i\,\text{detection}} * p_{i\,\text{spectrum}} * p_{\text{efficiency}})(m_{CCD})(t_{total})} \qquad (4)$$

We obtain an average rate in events/kg/day, by taking the weighted average of the results from the two search regions. This can be done using Equation 5:

$$\text{rate}_{avg} = \frac{(\text{rate}_1 * p_{1\,\text{detection}} * p_{1\,\text{spectrum}}) + (\text{rate}_2 * p_{2\,\text{detection}} * p_{2\,\text{spectrum}})}{(p_{1\,\text{detection}} * p_{1\,\text{spectrum}} + p_{2\,\text{detection}} * p_{2\,\text{spectrum}})} \qquad (5)$$

with the average error calculated the same way using appropriate rules of error propagation.

We can also use the average rate to calculate an average leakage rate ($\text{rate}_{leakage}$). This is the rate of ^{32}Si events we would expect to misclassify as ^{210}Pb events in an independent ^{210}Pb coincidence search. ^{210}Pb is a member of the ^{238}U decay chain and can remain as a long-term surface contaminant following exposure to environmental ^{222}Rn. Previous analysis has found indications of a significant amount of ^{210}Pb present on the surface of our CCDs [3]. Since the ^{210}Pb-^{210}Bi-^{210}Po decay chain also consists of two β decays, it can be analyzed using the same type of coincidence search we have described for the ^{32}Si-^{32}P decay chain except with an energy range of 0 - 70 keV and a time separation of 0 - 25 days to accord with the half-life and Q value of the ^{210}Pb decay (Table 1). This is why we avoid this region in our ^{32}Si analysis. However, we still expect ^{32}Si decays to occur at these energies and time scales. Thus, in order for future analysis to return an accurate estimate for the ^{210}Pb rate using a coincidence search, we must have an estimate for the rate of ^{32}Si decays we would expect to misclassify in such a search. This can be done using Equation 6:

$$\text{rate}_{leakage} = (\text{rate}_{avg})(p_{1\,\text{efficiency}} - p_{2\,\text{efficiency}})(p_{2\,\text{spectrum}}) \qquad (6)$$

where ($p_{1\,\text{efficiency}} - p_{2\,\text{efficiency}}$) accounts for the probability of decay in the 0 - 25 day region, and $p_{2\,\text{spectrum}}$ is used because we are considering decays that occur between 0 - 70 keV.

Table 3: Values Used for Coincidence Search

$p_{efficiency}$	89.9%
m_{CCD} (kg)	0.035
t_{total} (days)	273

	CCD	Module	Cable
^{238}U	0.005	0.057	0.372
^{226}Ra	0.007	0.252	0.115
^{210}Pb	——	1.994	——
^{232}Th	0.010	0.123	0.110
^{40}K	0.003	0.005	0.069
Activation	——	0.387	0.004
^{32}Si	0.238	——	——
^{3}H	3.018	——	——
^{22}Na	0.106	——	——

Table 4: decay rates in dru (events/kev/kg/day) for each of the detector parts and decay chains included in this analysis.

4 Results

4.1 Current Background

Table 4, shows the current background levels for the DAMIC at SNOLAB detectors based on the most up-to-date radioactivity measurements and Geant4 simulations. The rates in the table are all in events/kev/kg/day averaged over the energy range of 2 - 6 keV. This energy range is used because the spectrum for all isotopes currently under consideration is approximately flat in this region. As can be seen, in order to get the desired background rate of < 0.1 dru, significant background reduction will need to be done for DAMIC-M, especially with regards to ^{3}H, ^{32}Si, ^{210}Pb, ^{22}Na, copper activation in the module, ^{226}Ra and ^{232}Th in the cable and the module, and ^{238}U in the cable. ^{32}Si in the CCD can be reduced analytically, through a coincidence search like the one described in this paper. However, for the other decays, other methods will be required. Some can be reduced physically. In the cable, ^{226}Ra, ^{232}Th, and ^{238}U can be reduced through careful selection of construction materials, a problem which is being carefully considered for the current construction of DAMIC-M. Meanwhile, ^{3}H, ^{22}Na, and copper activation are all produced from cosmogenic activation of detector materials. Thus, these backgrounds can be reduced through careful shielding of the detector during the process of manufacture and transportation. Finally, the DAMIC-M copper modules will be machined out of electroformed copper rather than OFC copper. This should significantly reduce the ^{210}Pb, ^{232}Th, and ^{226}Ra backgrounds in the module.

4.2 Coincidence Search

From the analysis of the DAMIC at SNOLAB 1x100 data, number of events, number of accidentals, and decay rates for each of the two separate searches as well as the total values are displayed in Table 5. We find a total decay rate of 22.0 ± 6.1 events/kg/day. Previous analysis on the 1x1 data returned a slightly lower total decay rate of 11.5 ± 2.4 events/kg/day.

Looking at the results in Table 5, one can see that the discrepancy between these two rates comes from region 2. The current analysis returns a rate of 54.2 events/kg/day whereas the previous analysis measured a rate of 22.4 events/kg/day. This discrepancy could indicate an issue with how we reconstruct events in the 1x100 analysis. However, given the large error bars, these two measurements fall within 2σ of each other, so it is hard to determine whether this discrepancy is meaningful, or simply a result of statistical fluctuations.

	1x100			1x1
	n_{events}	$n_{accidentals}$	rate_{avg}	rate_{avg}
Region 1	159	134.4	11.6 ± 6.2	9.9 ± 2.6
Region 2	113	75.8	54.2 ± 16.0	22.4 ± 6.6
Total	272	210.2	22.0 ± 6.1	11.5 ± 2.4

Table 5: decay rates in events/kg/day measured in 1x100 vs 1x1 analysis

We can also measure the expected leakage of ^{32}Si leakage into the ^{210}Pb coincidence analysis. From our analysis, we return an expected leakage contribution of 2.8 ± 0.8 events/kg/day. This number will be useful in determining ^{210}Pb rates in future ^{210}Pb coincidence searches.

In order to compare the rate we measure through the coincidence search with the rate returned from the GUI analysis of the simulation spectra, we have to convert the rate from the coincidence search from events/kg/day to dru. This can be done using Equation 7:

$$\text{rate (dru)} = \frac{(\text{rate}_{avg})(p_{\Delta E\,\text{spectrum}})}{(\Delta E)} \tag{7}$$

where $p_{\Delta E\,\text{spectrum}}$ is the percentage of the total ^{32}Si β-decay energy spectrum accounted for in the energy range ΔE. For the 2 - 6 keV energy range this percentage value is approximately 3.7% [8] ($p_{\Delta E\,\text{spectrum}} = 0.037$) and $\Delta E = 4$ keV. Inputing these values, we return a rate in dru of 0.202 ± 0.056 from the coincidence search. This value is in very good agreement with the rate of 0.238 dru determined from the background simulation studies (Table 4). This is a strong indication that the coincidence search can be highly effective at detecting the ^{32}Si background.

5 The Future: DAMIC-M

While the focus of this work was on the analysis of data and simulations from DAMIC at SNOLAB, everything described here has been developed with an eye to its future applicability to the DAMIC-M experiment. Both the GUI and the coincidence search lay the groundwork for background handling in the next generation of DAMIC. Once simulations for DAMIC-M are complete, the GUI can be easily adapted as a tool for understanding those backgrounds. Furthermore, using the methods described here, we hope to be able to reduce the total radioactive backgrounds below the desired rate of 0.1 dru. For most of the components, we believe we can reduce these backgrounds physically, through a careful selection of materials and a controlled manufacturing process as described in Section 4.1. Meanwhile, for ^{32}Si, the coincidence search described in Section 3.2 can be used to reduce the background. Based on our current analysis, and assuming that the detection efficiency and overall background rates will remain approximately the same for DAMIC-M, reduction of the ^{32}Si rates by the predicted 89.9% efficiency should be achievable using a coincidence search. This would put the levels well below the desired 0.1 dru. Additionally, the agreement between the rates return from the 1x1 and 1x100 data, indicates that the loss of spatial information through pixel stacking does not significantly affect this type of analysis. This is promising, as for DAMIC-M we hope to readout the CCDs continuously, therefore completely losing spatial reconstruction in one direction. However, this analysis indicates that even in this readout regime, we will still likely be able to remove a significant portion of the ^{32}Si background through a coincidence search. Thus, this analysis, though focused on DAMIC at SNOLAB, is necessary to the process of planning, manufacture, and data analysis for DAMIC-M in order to achieve our desired sensitivity. It is therefore integral to the ultimate success of the experiment.

References

[1] Alain Blanchard and Monique Signore. *Frontiers of Cosmology: Proceedings of the NATO Advanced Study Institute on The Frontiers of Cosmology*. January 2005.

[2] A Aguilar-Arevalo, D Amidei, X Bertou, D Bole, M Butner, et al. The damic dark matter experiment. *arXiv preprint*, 2015.

[3] A. Aguilar-Arevalo, D. Amidei, X. Bertou, D. Bole, M. Butner, et al. Measurement of radioactive contamination in the high-resistivity silicon CCDs of the DAMIC experiment. *Journal of Instrumentation*, 10(08):P08014–P08014, August 2015.

[4] Meng Wang, G. Audi, F. G. Kondev, W.J. Huang, S. Naimi, et al. The AME2016 atomic mass evaluation (II). tables, graphs and references. *Chinese Physics C*, 41(3):030003, March 2017.

[5] Jagdish K. Tuli. Evaluated Nuclear Structure Data File and Related Products. *AIP Conf. Proc.*, 769(1):265, 2005.

[6] S. Agostinelli, J. Allison, K. Amako, J. Apostolakis, H. Araujo, et al. GEANT4: A Simulation toolkit. *Nucl. Instrum. Meth.*, A506:250–303, 2003.

[7] Rene Brun and Fons Rademakers. Root - an object oriented data analysis framework. In *AIHENP'96 Workshop, Lausane*, volume 389, pages 81–86, 1996.

[8] Michael Stabin and Lydia C Q P da Luz. Decay data for internal and external dose assessment. *Health physics*, 83:471–5, November 2002.